J Mater Sci (2008) 43:4979–4987
DOI 10.1007/s10853-008-2734-7

Fabrication and performances of epoxy/multi-walled carbon nanotubes/piezoelectric ceramic composites as rigid piezo-damping materials

Sheng Tian · Xiaodong Wang

Received: 23 February 2008 / Accepted: 16 May 2008 / Published online: 3 June 2008

Abstract Piezo-damping epoxy-based composites containing various amounts of multi-walled carbon nanotubes (CNT) and piezoelectric lead zirconate titanate (PZT) were prepared, and their performances were investigated. The composites exhibited a percolation threshold in the range of 1–1.5 g CNT per 100 g epoxy, in which a continuous electro-conductive network formed. Dynamic mechanical thermal analysis reveals that the loss factors of the composites were improved by incorporation of the PZT and the CNT at above critical electrical percolation loading. Based on this new type rigid piezo-damping material, the PZT contributes to the transformation of mechanical noise and vibration energies into electric energy, while the CNT serve in shorting of the generated electric current to the external circuit. Thermal stability and mechanical properties were also improved by incorporating these two fillers. An optimum formulation for the rigid piezo-damping materials can be designed on the basis of the results of this study.

Introduction

Damping materials have a good ability to dissipate elastic strain energy when subjected to vibratory loads, and they have been widely used in the fields of high-performance structural applications, such as aerospace, marine, aircraft, construction, automobile, skyscrapers, appliance industries, etc. [1, 2]. Polymers are the most useful damping materials; however, only the ones having the great loss factor and broad distribution of the molecular relaxation can be employed. In most cases, rubbers and rubber-based composites can match this requirement, which, to some extent, results in a limitation of the polymeric damping materials used in structural fields [3, 4]. In addition, the damping efficiency for polymeric materials is not very good. It is well known that the width and height of the loss peak for a given polymer cannot be independently adjusted, as the broadening of the loss peak usually results in a decrease in its maximum height. In fact, values of loss factor of good damping materials are higher than 0.3 in the range of temperature more than 60 °C. Moreover, once these materials and structures for damping are decided, their dynamic mechanical properties of the polymers cannot be changed. The interpenetrating polymer network (IPN) was considered as a possible ways of overcoming some of these problems [5, 6]. Owing to such properties of partial compatibility and broad distribution of the molecular relaxation for IPN, a broader temperature range of thermal transition can be obtained. Some IPN like polyurethane (PU)/polymethyl methacrylate, epoxy/acrylics, PU/epoxy, and unsaturated polyester/epoxy systems were reported as the good damping materials [7–10]. On the other hand, polymers usually cannot be used alone for high damping structural fields because of their limited properties such as poor mechanical properties, high shrinkage ratio and limited acclimatization. The polymer-inorganic composites have received great interest for their high specific strength, high modulus and lightweight, as well as good damping properties such as the fly ash filled epoxy composites that reported by Gu et al. [11, 12].

In recent years, a new damping material has been developed on the basis of a new damping mechanism. It can be described as follows: for some specialized composites,

S. Tian · X. Wang (✉)
Key Laboratory of Beijing City on Preparation and Processing of Novel Polymer Materials, School of Materials Science and Engineering, Beijing University of Chemical Technology, Beijing 100029, China
e-mail: wangxdfox@yahoo.com.cn

mechanical vibrating energy is first transmitted to the piezoelectric ceramic powders and converted into alternating electrical potential energy by the piezoelectric effect. Then, the electrical potential energy is further converted into joules heat through the networks of electro-conductive particles in polymeric matrix [13, 14]. For simplicity, such an energy transferring effect is rather hereafter referred to as the piezo-damping effect hereby. In order to obtain an electro-conductive polymeric matrix, carbon black or copper wires used typically as fillers are introduced into the polymers; however, high loadings required often have a negative effect on the mechanical properties of the matrix [15, 16]. High aspect ratio and highly conductive single- and multi-walled carbon nanotubes (CNT) are regarded as promising fillers, since they can provide electrical percolation at very low concentrations [17–19]. In terms of the experimental date, the multi-walled CNT rather than the single-walled ones have been predominantly used as electro-conductive fillers due to their lower cost, better availability and easier dispersibility [20]. On the other hand, a few literatures recently reported the electrorheological and the magnetrorheological characteristics for the composites containing CNTs, which implies that the CNTs could be applied potentially as smart damping materials under either electric or magnetic fields [21, 22].

In this article, we developed a novel type of epoxy-matrix composites with the multi-walled CNT and the piezoelectric lead zirconate titanate (PZT), which can be used as the rigid piezo-damping materials. Epoxy resins are well established as thermosetting matrices of advanced composites, displaying a series of promising characteristics for a wide range of application. The PZT is usually used as piezoelectric ceramic fillers to construct the piezoelectric units in the polymer matrix [13]. Through the PZT particles embedded in the epoxy matrix, the vibrational energy is changed into electric energy due to its piezoelectric effect and the electric energy is dissipated as thermal energy through an external electric resistance [23]. This may donate a good damping property to the rigid polymers like epoxy resins. The main aim of the present article is to fabricate and investigate the epoxy/CNT/PZT composites, and to discover their damping mechanisms.

Experimental

Materials

The epoxy resin (diglycidyl ether of bisphenol-A type) with an epoxide equivalent weight of 184–194 g/eq. was supplied by Wuxi Dic Epoxy Co., Ltd. China. 4,4′-Diaminodiphenylmethane (DDM) used as curing agent was purchased from Beijing Chemical Reagent Co., Ltd., China. The PZT ceramic was commercially supplied by the Institute of Acoustics, Chinese Academy of Sciences. The multi-walled CNT with diameters and average length respectively in the ranges of 60–100 nm and 5–10 μm was purchased from Shenzhen Nanotech Port Co., Ltd.

Preparation of the composites

The PZT plates were electrically polarized along the thickness direction in silicone oil at 7 kV/mm and 110 °C for 20 min, and then were milled to the particles with the mean particle size of about 5–10 μm. The PZT and the CNT was surface-treated, respectively, with 3-glycidyl-oxypropyl trimethoxysilane and with a mixed alkaline solution containing H_2O_2/NH_4OH (28.5 wt.%) before use, so that the fillers can be functionalized with amino groups. The composites were prepared by thermosetting process as follows: The CNT and PZT particles were first dispersed in acetone together under an ultrasonic agitation at room temperature for 30 min. In addition, a well-mixed epoxy resin and curing agent was added to the mixture for another 30 min under ultrasonic agitation. In succession, the suspensions were stirred for 1 h at 2,000 rpm. During these stage, the temperature of the resin was kept at 60 °C using a silicone bath to maintain a low viscosity of the resin so as to make the fillers dispersed adequately. In order to evaporate the acetone solvent, the mixtures were kept in a vacuum oven at 50 °C for 1 h. A three-stage thermal curing procedure was carried out at 80 °C for 2 h, 120 °C for 2 h and 150 °C for 3 h.

Characterizations

Measurements of electrical conductivity

Electrical conductivities were measured by using an Agilent-4294A impedance/gain phase analyzer with a voltage-amplitude of 0.5 V_{AC} at a frequency of 1 MHz. The testing specimens were prepared with 12 mm in diameter and 1.2 mm in thickness through polishing and electroplated by silver-paint on both sides. Dielectric constants were measured on a WY2851-type LCR bridge meter (manufactured by Shanghai Wuyi Electronics Co., Ltd.) at a frequency of 1 MHz.

Measurements of damping properties

The damping properties were evaluated by dynamic mechanical thermal analysis (DMTA) using a Rheometric Scientific V dynamic mechanical analyzer with three point bending mode over the temperature range from 10 to 220 °C at a heating rate of 5 °C min^{-1}. The frequency and the strain were set to 1 Hz and 0.5%, respectively. The specimen size was 50 × 6 × 2 mm^3 in length, width, and thickness, respectively.

Scanning electronic microscopy

Scanning electron microscopy (SEM) was performed on a Hitachi S-4700 scanning electron microscope, and morphologies of the impact-fractured surfaces of the composites were determined from SEM images. The brittle impact-fractured surfaces of the composites were obtained through an impacted fracture in liquid nitrogen and mounted on the sample stud by means of a double-sided adhesive tape for cross-sectional view study. A thin layer of gold was sputtered onto the cross-sectional surface prior to SEM observation.

Measurements of thermal properties

The Perkin-Elmer Pyris-1 differential scanning calorimeter was used to measure the differential scanning calorimetry (DSC). All measurements were made under an N_2 atmosphere at a heating rate of 10 °C/min on samples weighing about 10 mg. Thermal gravimetric analysis (TGA) was carried out on a Perkin-Elmer Pyrid-1 thermal gravimetric analyzer at a heating rate of 10 °C min^{-1} from 50 to 220 °C under an N_2 atmosphere.

Measurements of mechanical properties

The impact and tensile test bars were fabricated via a cast molding. Charpy impact strength was measured with a SUMITOMO impact machine tester according to a Chinese national standard of GB/T1043-98. The thickness of the Charpy impact specimen was 4 mm, and impact energy was 4 J. The tensile properties were determined with an Instron-1185 universal testing instrument using a 1000 Newton load transducer according to a Chinese national standard of GB/T1040-98. Small dumb-bell specimens with waist dimensions of 20 × 4 mm^2 were used for tensile mechanical tests. All the tests were done at room temperature and five measurements were carried out for each data point.

Results and discussion

Electrical properties

The electrical conductivities of all samples as a function of CTN loading are summarized in Fig. 1. As expected, the epoxy/CNT composites show a percolation behavior in electrical conductivity with increasing CNT loading. The electrical conductivities of these binary composites increase abruptly over the range from 0.3 to 1.0 g CNT per 100 g epoxy, indicating a percolation threshold of around 0.8 g CNT per 100 g epoxy. The composite with the CNT loading of 1.5 g per 100 g epoxy has an electrical conductivity of around 10^{-3} S m^{-1}, which is 10^{10} times higher than that of

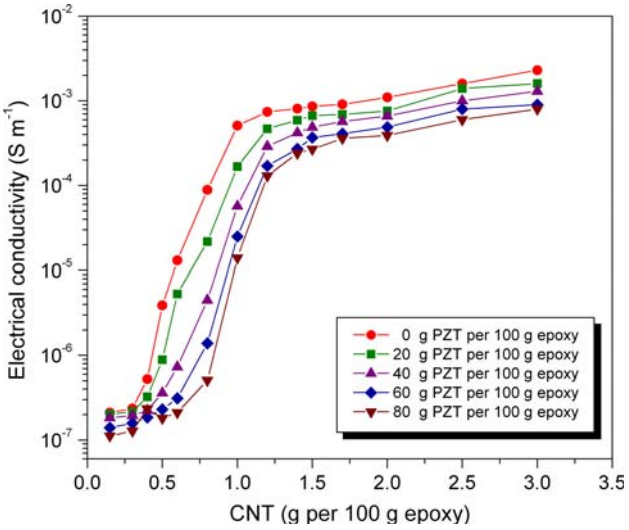

Fig. 1 Electrical conductivity as a function of PZT loading for the composites

the pure epoxy (around 10^{-13} S m^{-1}). It is understandable that the epoxy-matrix composites with a CNT loading above the critical electrical percolation have the conductive path of continuous interconnected nanotubes that allow electrons to travel. The high aspect ratio of CNT allows reaching such a conductive threshold with a small CNT fraction.

An electron hopping mechanism has been adopted to describe the electrical conductivity of nanotube/polymer nanocomposites [24, 25]. This mechanism requires close proximity (<5 nm) of the nanotubes or nanotube bundles in the nanocomposites and direct nanotube contact is unnecessary. It is also noticeable (see Fig. 1) that the electrical conductivities of epoxy/CNT/PZT composites exhibit a similar variational trend with increasing CNT loading. However, their values reduce in comparison with the binary composites with same CNT loading, and the percolation thresholds also shift to higher CNT loading with increasing the PZT loading. It is well known that, for the polymer/CNT composites, there is a contact resistance existing between the CNT (or clusters of the CNT) in polymer matrix, which reduces the effective conductivity of the CNT themselves. After incorporating the PZT particles into the epoxy/CNT composites, two neighboring conductive clusters are separated not only by the insulating epoxy resin but also by the insulating PZT particles. This results in much lower electrical conductivities of the binary composites than those of the ternary ones with the same CNT loading.

Figure 2 shows the dependence of the dielectric constant on the PZT loadings, indicating that the improved dielectric constants of the composites with increasing the PZT loading are due to the electron domain orientation in the ceramic phases. The dielectric constant of a material is a function of its capacitance, which is proportional to the number of charges stored on either surface of the sample under an

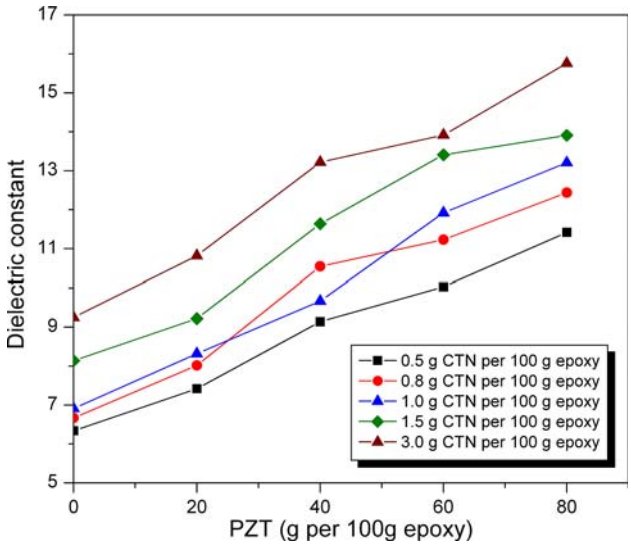

Fig. 2 Dielectric constant as a function of PZT loading for the composites

applied electric field. When an electric field is imposed on composites, the composites become polarized and the numbers of the accumulated charge will increase because of the electron domain orientation in the ceramic phases [25]. In addition the contribution of orientation polarization is proportional to the PZT loading. The results also suggest that the main contribution to dielectric behavior comes from the ceramic phase in polymer/ceramic composites.

Morphology

Figure 3 displays the SEM images for the impact-fractured surface of the epoxy/CNT binary and epoxy/CNT/PZT ternary composites. A good dispersion can be deduced from the pattern of the fracture surfaces of these samples, in which the original traces of the imbedded CNT can be clearly distinguished. Figure 3a shows the fracture surface of the binary composites with the CNT loading of 0.5 g per 100 g epoxy. This image confirms that individual

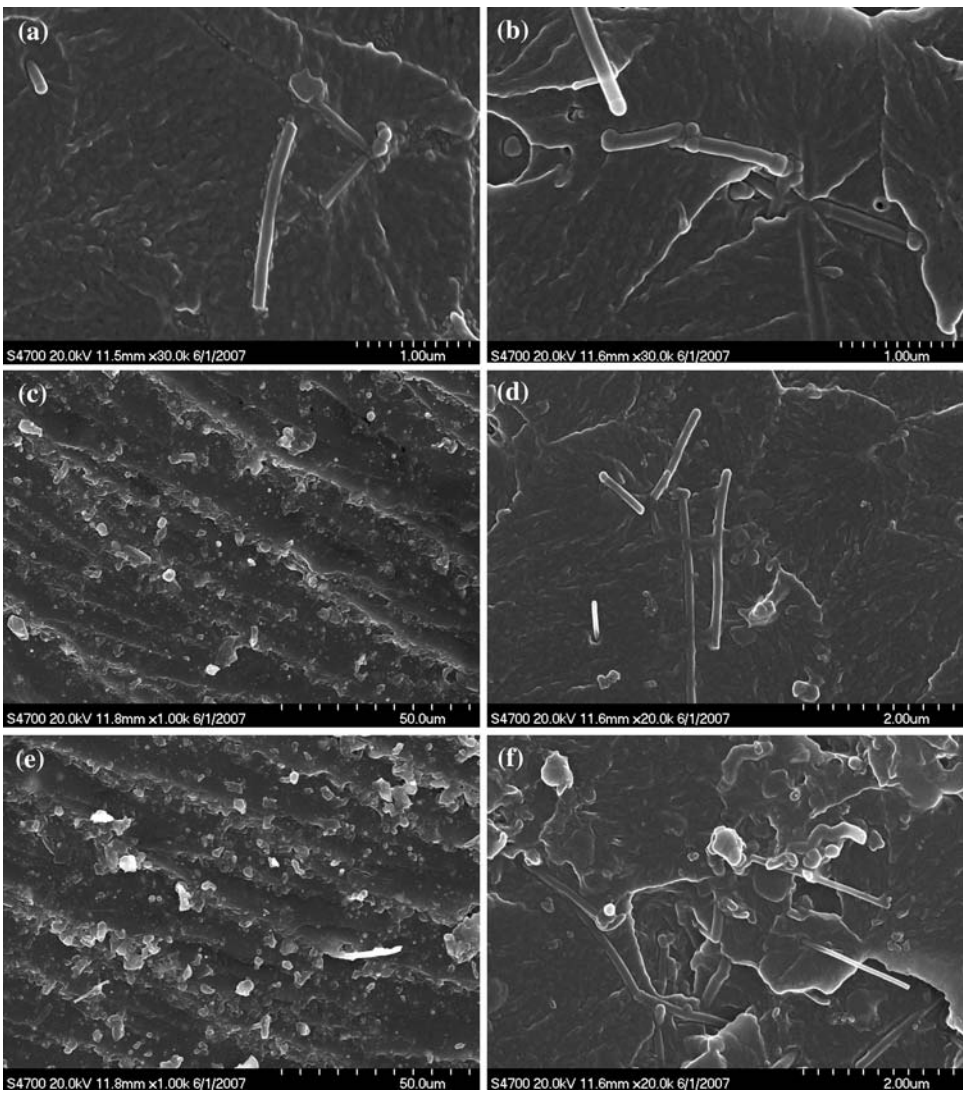

Fig. 3 SEM images of the composites containing (**a**) 0.5 g CNT per 100 g epoxy, (**b**) 1.5 g CNT per 100 g epoxy, (**c**, **d**) 0.8 g CNT, and 20 g PZT per 100 g epoxy, and (**e**, **f**) 1.5 g CNT, and 40 g PZT per 100 g epoxy

nanotubes are dispersed during processing of these composites. Furthermore, at a higher loading of 0.5 g per 100 g epoxy, and contacts between adjacent nanotubes are observed to occur, and no aggregation is seen as shown in Fig. 3b. These images highlight the transition from a dispersed state to an interconnected network of the CTN as a function of concentration and are in agreement with the results of the electrical conductivity measurements.

A very good dispersion of the PZT particles is also observed in matrix in a large field of vision from the fracture surfaces of the epoxy/CNT/PZT ternary composites as shown in Fig. 3c and e indicating a good interfacial adhesion between the PZT and the epoxy. The much higher magnification SEM images shown in Fig. 3d and f give an insight of the nanoscale morphology, in which the dispersion of the CNT could be clearly distinguished. The fracture process did not follow the CNT or the PZT particles pullout pattern and the cracks propagated along the plane of the nanotube mesh, indicating a good interfacial adhesion between the CNT (or PZT) and the epoxy matrix. It is also noticed that there are fewer contacts between adjacent nanotubes and less CNT loading makes less contribution to formation of the conducting network in Fig. 3d. However, the conductive networks have formed when the CNT loading reaches 1.5 g per 100 g epoxy (see Fig. 3f).

Dynamic mechanical analysis

Figure 4 illustrates the dynamic mechanical spectra of the composites in term of the storage and the loss moduli as a function of temperature. The incorporation of the CNT and PZT to epoxy resin induces a positive influence on the storage modulus both in the glassy region and in the vicinity of the glass transition temperature (T_g). The addition of these fillers improves its elastic properties of the epoxy system. The behavior can be attributed to the presence of the fillers, which reduces free volume and hinders motion of the molecules of the epoxy matrix. Furthermore, owing to the surface modification for fillers, a good interfacial interaction reduces the mobility of the epoxy matrix around the fillers and leads to the observed increase in thermal stability. This effect will become stronger around and above T_g, due to the limited potential movement of the polymeric matrix below. The storage modulus also shifts to higher temperature and increases with increase of the PZT loading. It is also observed that the loss modulus presents a significant improvement as a result of the continuous increase of the PZT loading. The dispersed fillers not only dissipate energy due to resistance against viscoelastic deformation of the surrounding epoxy matrix, but the piezo-damping effect also begins to works in the system as discussed in the following paragraph, leading to much more energy dissipated in the composites.

Loss factor (tanδ) is an important parameter characterizing macromolecular viscoelasticity, and also represents damping capacity of the materials that expresses an ability of converting the mechanical energy into heat energy when the material is subjected to an external loading [12, 26]. It is generally defined as $\tan\delta = E''/E'$, where tanδ is the phase angle between stress and strain, E' the elastic storage modulus and E'' the elastic loss modulus. Figure 5 shows the temperature dependence of loss factor for the composites. It can be found that the pure epoxy presents a low value of the loss factor at working temperature of around 25 °C. This suggests its low damping capacity. We cannot find any improvement in loss factor for the epoxy/CNT/PZT (100/0.5/2) composites at room temperature, indicating the lower CNT loading makes the epoxy an electrical

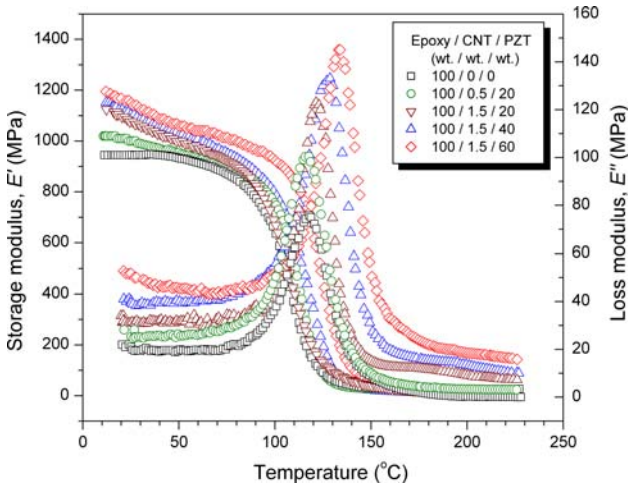

Fig. 4 Temperature dependences of storage and loss moduli for the composites

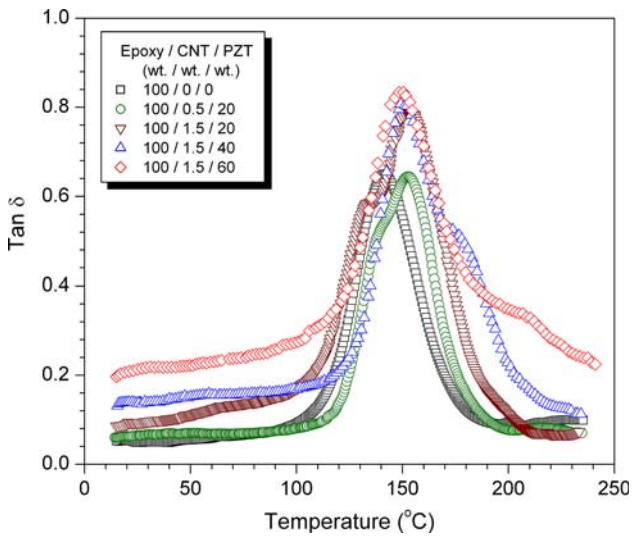

Fig. 5 Temperature dependence of loss factor for the composites

insulator, and here the electric energy generated from the PZT is not fully dissipated. However, when the CNT loading rises up to 1.5 g per 100 g epoxy, the loss factor exhibits a fair increment. Apparently, the higher CNT loading causes formation of electro-conductive network in the composite, and the generated electric current flows throughout the composite. As a result, the electric energy is well dissipated, and the piezo-damping effect begins to work in the systems. Moreover, it is found that, from the dependences of the loss factor on the PZT loading at room temperature as shown in Fig. 6, the loss factor is improved with increasing the PZT loading, indicating that the higher PZT loading can make more mechanical energy be converted into electrical energy and the electrical energy is dissipated as heat in a load resistance. It is also found that, when the CNT loading ranges within 1–1.5 g per 100 g epoxy, the generated electrical energy is well dissipated. However, when their loadings exceed the percolation threshold significantly, the CNT fully contact each other and may act rather as electric conductors. The CNT contribute to the increase of the loss factor only through the electric shorting of the electric energy generated by PZT particles to the external circuit. As a result, the electric energy is not fully dissipated, and the piezo-damping effect becomes weak.

From Fig. 5, it can also be seen that the loss factor of the composites exhibits the same variation trends as that of the pure epoxy resin are greatly affected by the operating temperature. The loss factor varies with increasing temperature and achieves a maximum value corresponding to the T_g. For polymers and their composites, damping capacity is quite sensitive to the operating temperature because their intrinsic damping is the matrix viscoelasticity, which is one typical behavior of polymeric materials [27]. At around T_g of the given polymer, the peak intensity of loss factor is directly related to the coordinated chain molecular friction, which dissipates mechanical energy as heat. Moreover, the frictions caused by the particle boundary sliding (filler–filler) and the interfacial sliding (filler–matrix) are all thermally activated [28]. It also should be noted that the addition of fillers like the CNT and the PZT has a profound effect on the terminal relaxation time of the composites. With increasing filler loading, the liquidlike relaxation observed for the pure polymer gradually changes to solidlike (or pseudo-solidlike) behavior for the composites [29]. At this temperature region, the piezo-damping effect is not obvious, as the mechanical vibration energy converts into thermal energy is higher, because of the frictions within the epoxy matrix. Therefore, the loss factor can only reach peak values at the T_g of such composites. For the temperature dependence of the loss factor of the composites at the temperature much higher than T_g, and the contribution of the matrix viscoelasticity to composites damping is regnant, so the piezo-damping effect is not obvious.

Thermal properties

The T_g is a very important parameter of thermal properties for the epoxy-based composites, because it established the service environment for these materials. In most cases, epoxy-based composites are only used well at a temperature below T_g. Therefore, identification of the mechanisms responsible for T_g changes and prediction of T_g depression are critical for the engineering design and the application of epoxy-based composites. Figure 7 displays the DSC thermograms of the epoxy-matrix composites with CNT and PZT, in which their T_gs are clearly distinguished and

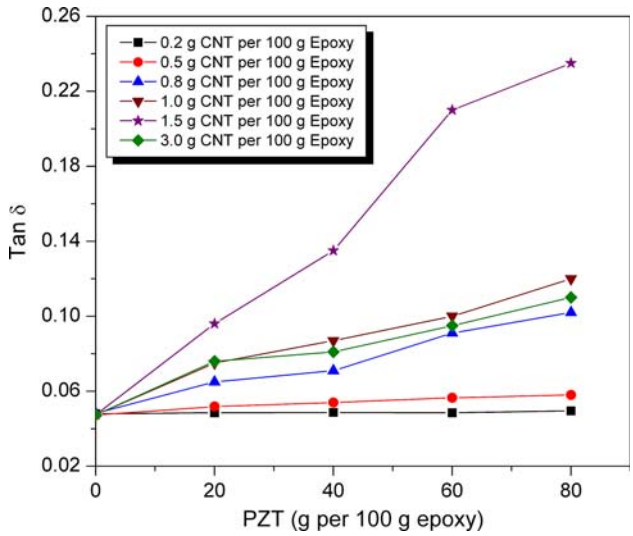

Fig. 6 Loss factor as a function of PZT loading at room temperature for the composites

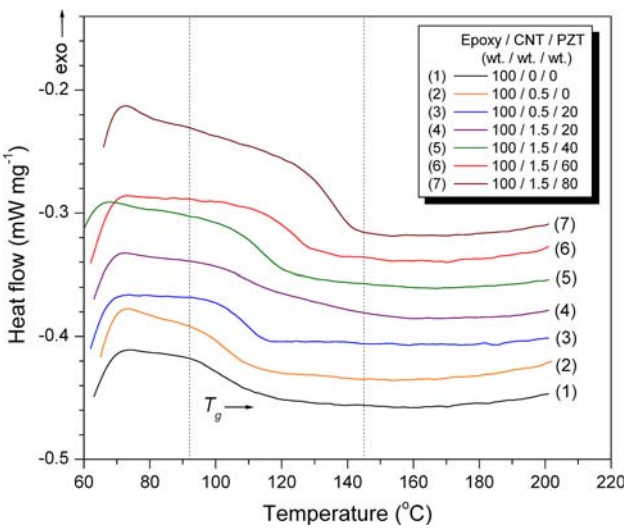

Fig. 7 DSC thermograms for the epoxy/CNT/PZT composites

Table 1 Thermal analysis experimental data of the epoxy/CTN/PZT composites

Samples epoxy/CTN/PZT (wt.%/wt.%/wt.%)	T_g (°C)	Temperature at characteristic weight loss (°C)		Temperature at rapid weight loss (°C)	Char ratios at 750 °C (wt.%)
		1 wt.%	10 wt.%		
100/0/0	102.3	197.2	315.1	415.5	6.8
100/0.5/0	102.7	198.5	315.4	417.3	7.2
100/0.5/20	108.5	202.2	317.6	420.1	17.4
100/1.5/20	111.9	204.9	317.8	423.5	18.2
100/1.5/40	116.2	206.7	319.6	427.9	32.5
100/1.5/60	125.6	209.5	322.7	430.2	40.7
100/1.5/80	132.8	210.4	324.2	434.3	47.6

summarized in Table 1. It is observed that all composites exhibit higher T_gs than that of the pure epoxy, and a shift of T_gs to higher temperatures occurs with a continuous increase of the PZT loading. Considering an effective surface modification for CNT and PZT, an improved interfacial interaction between the inorganic and organic domains increases the motional and rotational barriers of the epoxy molecules. The incorporation of fillers also forms the physical hindrance, which impairs the mobility of the epoxy molecules, thus resulting in a significant improvement in the T_gs of the composites [30].

The effects of CNT and PZT on the thermal degradation of the epoxy-based composites were investigated by using TGA. TGA thermograms presenting the thermal degradation behaviors of these composites are shown in Fig. 8, and the obtained data are summarized in Table 1. It is found that the thermal degradation of all the samples performs in the programmed temperature range of 50–800 °C and occurs through one degradation step in this temperature range, indicating a good phase interconnection between fillers and epoxy matrix. TGA thermograms also indicate that water or solvent has been successfully removed from the resins and the composites because there is no weight loss below 100 °C. It is clearly suggested that the thermal stability of the epoxy is improved by incorporation of the fillers in terms of the temperatures at primary decomposition and at rapid weight loss, and the weight percent of the residues above 750 °C. The increase in these three parameters suggests that the incorporation of CNT and PZT into the epoxy results ultimately in an improvement in thermal stability. This improvement mainly comes from the enhanced interaction between epoxy matrix and fillers [31]. Furthermore, it may also be assumed that the thermal stability of organic materials can be improved by introducing inorganic components on the basis of the fact that these materials have inherently good thermal stability [32].

Mechanical properties

The impact strength and tensile strength of epoxy/CNT/PZT composites as a function of the PZT loading are displayed in Figs. 9 and 10, indicating that the incorporation of these two fillers into epoxy resin has significant effects on the mechanical properties. The pure epoxy resin suggests a typical brittle plastic behavior with low impact strength of 4.6 kJ/m^2 and moderate tensile strength of 34.8 MPa. It is noteworthy that both impact and tensile strengths of the composites increases significantly with addition of the CNT and the PZT. The mechanical properties reach maximum values at the PZT loading of 40 g per 100 g epoxy, followed a drop with a continuous increase of the PZT loading. It is evident that the toughening effect of the PZT could be explained by the crack front bowing mechanism [33, 34]. For

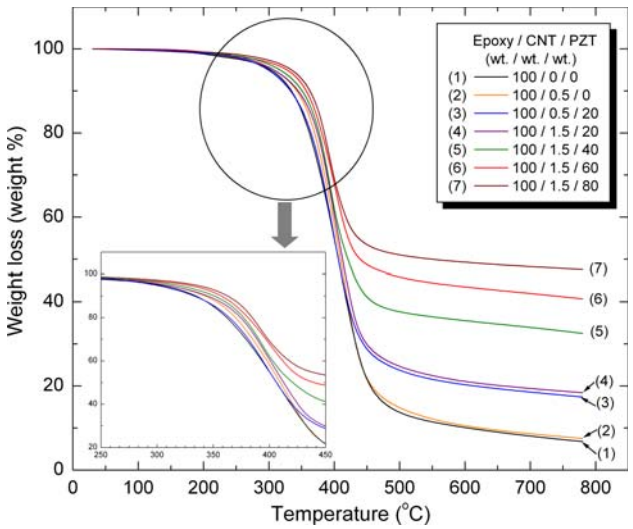

Fig. 8 TGA thermograms for the epoxy/CNT/PZT composites

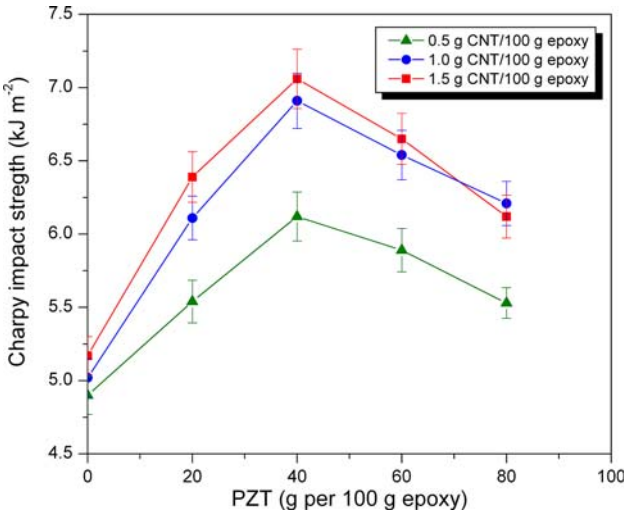

Fig. 9 Impact strength of the epoxy/CNT/PZT composites as a function of PZT loading

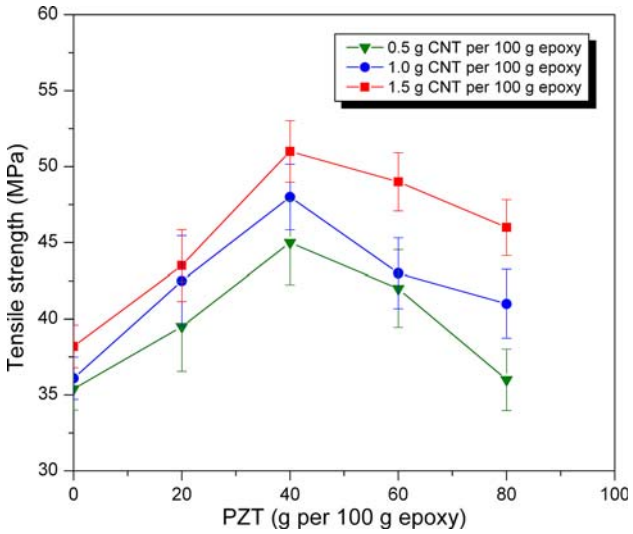

Fig. 10 Tensile strength of the epoxy/CNT/PZT composites as a function of PZT loading

the toughening polymer system using inorganic particles, the rigid particles can resist the propagation of the crack, so the primary crack has to bend between the neighboring particles. However, high PZT loading dominates a natural incompatibility of the inorganic and organic domains, and thus, results in a reduction in toughness [35–37]. Poor stress transfer also leads to a deterioration of the tensile strength. On the other hand, the surface-modified CNT also plays a role of efficient reinforcement in the epoxy resin on the basis of a good interfacial interaction between two domains as reported in literatures [38]. As expected, the composites with higher CNT loading present much better tensile strengths under a condition of the same PZT loading.

Conclusion

A new type of the piezo-damping epoxy-based composites with CNT and PZT was developed in this article. The piezo-damping effect is obvious for the epoxy-based composites with high PZT loading and CNT at above critical electrical percolation loadings. The thermal stability and the mechanical properties as well as the dielectric constants were also improved by incorporating these two fillers. The present work provided a useful route to design a good piezoelectric damping material, in which PZT contributes to the transformation of mechanical noise and vibration energies into electric energy, while CNT serve in shorting of the generated electric current to the external circuit. Based on the results of this study, an optimum formulation for the piezo-damping epoxy-based materials is designed.

Acknowledgement The authors greatly appreciated financial supports from the National Natural Science Foundation of China (Grant No. 50573006).

References

1. Vinogradov AM, Schmidt VH, Tuthill GF, Bohannan GW (2004) Mech Mater 36:1007. doi:10.1016/j.mechmat.2003.04.002
2. Rajoria H, Jalili N (2005) Compos Sci Technol 65:2079. doi:10.1016/j.compscitech.2005.05.015
3. Zhang C, Sheng JF, Ma CA, Sumita M (2005) Mater Lett 59:3648. doi:10.1016/j.matlet.2005.07.004
4. Kang S, Hong SI, Choe CR, Park M, Rim S, Kim J (2001) Polymer (Guildf) 42:879. doi:10.1016/S0032-3861(00)00392-X
5. Chandra R, Singh SP, Gupta K (1999) Compos Struct 46:41. doi:10.1016/S0263-8223(99)00041-0
6. Salamone JC (1996) Encyclopedia of polymeric materials. CRC Press, New York
7. Shih YF, Jeng RJ (2002) J Appl Polym Sci 86:1904. doi:10.1002/app.11145
8. Chen Q, Ge H, Chen D, He M, Yu X (1994) J Appl Polym Sci 54:1191. doi:10.1002/app.1994.070540901
9. Lin MS, Lee ST (1997) Polymer (Guildf) 28:53. doi:10.1016/S0032-3861(96)00484-3
10. Hsieh KH, Chiang YC, Chen YC, Chiu WY, Ma CCM (1992) Angew Makromol Chem 194:15. doi:10.1002/apmc.1992.051940102
11. Gu J, Wu G, Zhang Q (2007a) Scr Mater 57:529. doi:10.1016/j.scriptamat.2007.05.019
12. Gu J, Wu G, Zhang Q (2007b) Mater Sci Eng A 452:614. doi:10.1016/j.msea.2006.11.006
13. Horia M, Aokia T, Ohiraa Y, Yano S (2001) Compos Part A Appl Sci Manuf 32:287. doi:10.1016/S1359-835X(00)00141-X
14. Yan X, Zhang H, Sumita M (2001) J Dong Hua Univ Eng Ed 18:11
15. Liao YH, Marietta-Tondin O, Liang Z, Zhang C, Wang B (2004) Mater Sci Eng A 385:175. doi:10.1016/j.msea.2004.06.031
16. Lv L, Bai S, Zhang H, Wang J, Yang J, Xiao J (2006) Mater Sci Eng A 433:121. doi:10.1016/j.msea.2006.06.031
17. Bryning MB, Islam MF, Kikkawa JM, Yodh AG (2005) Adv Mater 17:1186. doi:10.1002/adma.200401649
18. Kim YJ, Shin TS, Choi HD, Kwon JH, Chung YC, Yoon HG (2005) Carbon 43:23. doi:10.1016/j.carbon.2004.08.015
19. Allaoui A, Bai S, Cheng HM, Bai JB (2002) Compos Sci Technol 62:1993. doi:10.1016/S0266-3538(02)00129-X
20. Thostenson ET, Chou TW (2006) Carbon 44:3022. doi:10.1016/j.carbon.2006.05.014
21. Kim ST, Lim JY, Park BJ, Choi HJ (2007) Macromol Chem Phys 208:514. doi:10.1002/macp.200600543
22. Fang FF, Choi HJ (2008) J Appl Phys 103:07A301
23. Law HH, Rossiter PL, Koss LL, Simon GP (1995) J Mater Sci 30:2648. doi:10.1007/BF00362148
24. Gojny FH, Wichmann MHG, Fiedler B, Kinloch IA, Bauhofer W, Windle AH et al (2006) Polymer (Guildf) 47:2036. doi:10.1016/j.polymer.2006.01.029
25. Nan CW, Shi Z, Lin Y (2003) Chem Phys Lett 375:666. doi:10.1016/S0009-2614(03)00956-4
26. Liang JZ, Li RKY, Tjong SC (2000). Polym Test 19:213. doi:10.1016/S0142-9418(99)00005-7
27. Tsantzalis S, Karapappas P, Vavouliotis A, Tsotra P, Paipetis A, Kostopoulos V et al (2007) Compos Part A Appl Sci Manuf 38:1076. doi:10.1016/j.compositesa.2006.04.015
28. Gu JH, Zhang XN, Gu MY, Gu M, Wang XK (2004) J Alloy Comp 372:304. doi:10.1016/j.jallcom.2003.10.021
29. Hyun YH, Lim ST, Choi HJ, Jhon MS (2001) Macromolecules 34:8084. doi:10.1021/ma002191w
30. Liu H, Zhang W, Zheng S (2005). Polymer (Guildf) 46:157. doi:10.1016/j.polymer.2004.10.078
31. Bauer F, Decker U, Ernst H, Findeisen M, Langguth H, Mehnert R et al (2006) Int J Adhes 26:567. doi:10.1016/j.ijadhadh.2005.11.001

32. Wen JY, Wilkes GL (1996) Chem Mater 8:1667. doi:10.1021/cm9601143
33. Sandler JKW, Kirk JE, Kinloch IA, Shaffer MSP, Windle AH (2003) Polymer (Guildf) 44:5893. doi:10.1016/S0032-3861(03)00539-1
34. Sandler JKW, Shaffer MSP, Prasse T, Bauhofer W, Schulte K, Windle AH (1999) Polymer (Guildf) 40:5967. doi:10.1016/S0032-3861(99)00166-4
35. Argon AS, Cohen RE (2003) Polymer (Guildf) 44:6013. doi:10.1016/S0032-3861(03)00546-9
36. Bartczak Z, Argon AS, Cohen RE, Weinberg M (1999) Polymer (Guildf) 40:2347. doi:10.1016/S0032-3861(98)00444-3
37. Thio YS, Argon AS, Cohen RE, Weinberg M (2002) Polymer (Guildf) 43:3661. doi:10.1016/S0032-3861(02)00193-3
38. Wang J, Fang Z, Gu A, Xu L, Liu F (2006). J Appl Polym Sci 100:97. doi:10.1002/app.22647